Elsevier Editorial System(tm) for Geoderma
Manuscript Draft

Manuscript Number:

Title: A Coupled Carbon, Aggregation, and Structure Turnover (CAST) Model for topsoils

Article Type: Research Paper

Section/Category: Soil Physics, Mechanics and Hydrology

Keywords: C/N sequestration; aggregation; structure; particulate OM; RothC; calibration.

Corresponding Author: Mrs Fotini E Stamati, PhD candidate

Corresponding Author's Institution: Technical University of Crete

First Author: Fotini E Stamati, PhD candidate

Order of Authors: Fotini E Stamati, PhD candidate; Nikolaos P Nikolaidis, Professor; Steven Banwart, Professor; Winfried E Blum, Professor

Abstract: The current multi-pool soil organic carbon (SOC) models, although a major improvement over the single pool ones, are not always able to capture soil saturation capacity and give reliable predictions for climate change effects, since they do not account for environmental constraints, like physical protection. In this work, we developed a soil carbon, aggregation, and structure (CAST) turnover model based on the concept suggested by many authors in the scientific literature that macro-aggregates are formed around particulate organic matter, followed by the release of micro-aggregates. A simplified mechanistic Nitrogen model was also developed. The CAST model was evaluated by field data of cropland to set aside conversions of Critical Zones Observatories in Greece (fine textured Mediterranean) and Iowa (coarse textured humid continental). The model was able to capture the carbon content and the C-to-N ratio content of the pools comprising the three aggregate types (macro-aggregates: >250 μm, micro-aggregates: 53-250 μm, silt-clay sized aggregates: <53 μm) in both sites. The soil system reached maximum macro-aggregation/porosity and minimum bulk density after 7 and 14 years in Greece and Iowa, respectively. Afterwards, macro-aggregate disruption presented a constant seasonal pattern and any further SOC increase was due to micro-aggregation resulting in the increase of bulk density and decrease of porosity towards to a stable value. The CAST model can assist in revealing primary factors determine organic matter, aggregation, and structure turnover in different ecosystems and in describing the response of the soil system to management practices, land use changes, and climate change in order to design and optimize the appropriate measures/practices.

A Coupled Carbon, Aggregation, and Structure Turnover (CAST) Model for topsoils

Fotini E. Stamati[a], Nikolaos P. Nikolaidis*[a], Steven Banwart[b], Winfried E.H. Blum[c]

[a]Department of Environmental Engineering, Technical University of Crete (TUC), University Campus, 73100, Chania, Greece, [b]Kroto Research Institute, North Campus, University of Sheffield, Sheffield S3 7HQ, UK, [c]University of Natural Resources and Life Sciences (BOKU), Vienna, Peter-Jordan-Str. 82, 1190 Vienna, Austria.

*corresponding author, Tel:+302821037831; Fax:+302821037847;

e-mail: fotini.stamati@enveng.tuc.gr

ABSTRACT

The current multi-pool soil organic carbon (SOC) models, although a major improvement over the single pool ones, are not always able to capture soil saturation capacity and give reliable predictions for climate change effects, since they do not account for environmental constraints, like physical protection. In this work, we developed a soil carbon, aggregation, and structure (CAST) turnover model based on the concept suggested by many authors in the scientific literature that macro-aggregates are formed around particulate organic matter, followed by the release of micro-aggregates. A simplified mechanistic Nitrogen model was also developed. The CAST model was evaluated by field data of cropland to set aside conversions of Critical Zones Observatories in Greece (fine textured Mediterranean) and Iowa (coarse textured humid continental). The model was able to capture the carbon content and the C-to-N ratio content of the pools comprising the three aggregate types (macro-aggregates: >250 μm, micro-aggregates: 53-250 μm, silt-clay sized aggregates: <53 μm) in both sites. The soil system reached maximum macro-aggregation/porosity and minimum bulk density after 7 and 14 years in Greece and Iowa, respectively. Afterwards, macro-aggregate disruption presented a constant seasonal pattern and any further SOC increase was due to micro-aggregation resulting in the increase of bulk density and decrease of porosity towards to a stable value. The CAST model can assist in revealing primary factors determine organic matter, aggregation, and structure turnover in different ecosystems and in describing the response of the soil system to management practices, land use changes, and climate change in order to design and optimize the appropriate measures/practices.

Keywords: C/N sequestration, aggregation, structure, particulate OM, RothC, calibration

1. Introduction

The current multi-pool soil carbon models have been a major improvement over the single pool ones (Davidson and Janssens, 2006). However, they are not always able to capture the soil saturation capacity to bind carbon (Powlson et al., 2011) and give reliable predictions for land use changes, management practices, and climate change effects, since they do not account for environmental constraints, like physical protection (Davidson and Janssens, 2006, Kleber and Johnson, 2010). Six et al. (2002a) acknowledged that one of the major knowledge gaps and a research priority is the mechanistic explanation of the saturation capacity level. Van Veen and Paul (1981), long ago have recognized that the equilibrium level of soil organic carbon (SOC) is more dependent on the extent of protection than on the decomposition rate of the plant residues added to soil.

Most models were designed based on the assumption that biochemically protected carbon contributing to humus, inert or passive pools was the product of the humification process resulting in a very stable highly aromatic material (Kleber and Johnson, 2010). Aromatic structures found in stable materials are the products of incomplete combustion (biochar) and are not the result of the natural decomposition process (Knicker, 2007; Baldock, 2007; Kleber and Johnson, 2010). The combination of physical fractionations (aggregate, particle size, and density fractions) with various chemical and spectroscopic methods for the chemical characterization of these fractions, have offered evidence and insight for the formulation of a more mechanistic conceptualization of soil organic matter (SOM) turnover, composition and stabilization (see reviews of Lützow et al., 2007 and Grandy and Neff, 2008). An updated concept of the dynamic nature of SOM is the realization that accessibility and

sorbtion interactions with mineral surfaces may provide powerful protection against decomposition, explicitly including carbohydrates, proteins and other 'labile' materials (Kleber and Johnson, 2010). Stabilization of SOM is thought to be due to (see also paragraph 1.2.4): 1) stabilization by organo-mineral interactions-association with silt and clay (OM that is absorbed to minerals or entrapped in very small micro-aggregates) and 2) physical protection within macro-aggregate and micro-aggregate structures (Six et al., 2002a; Six et al., 2002b).

Physical protection in SOM turnover has been included in models using simplified parameterization such as reduced life-time, protection coefficient or periodically transferred to a more labile pool during cultivation events (Van Veen and Paul, 1981; Molina et al., 1983). Hassink and Whitmore (1997) developed a model where the rate at which organic matter became protected depended on the degree to which the protective capacity was filled, incorporating the processes of desorption and adsorption in order to model silt and clay protection of SOM. Most of the current models of SOM dynamics simply affect the decay rates of SOM pools by an empirical parameter corresponding to land use. Recently, Malamoud et al. (2008) made the assumption that the primary interactions occur between clay particles and SOC components to form organo-mineral associations, which were then bound together to form aggregates (STRUC-C model). Even though STRUC-C has significant limitations, as outlined by the authors, it is the most comprehensive attempt to model soil aggregate stability and turnover as well as soil structure in the scientific literature thus far (Nikoalidis and Bidoglio, 2011; Adams et al., 2011). The STRUC-C model considered each aggregate type as being a single carbon pool and did not account for particulate organic matter (POM) in the aggregation process; the DPM (Decomposable Plant Material) and RPM (Resistant Plant Material) RothC carbon pools. In addition,

the formation of macro-aggregates (>250 μm) was considered as the aggregation product of micro-aggregates (>53-250 μm), although macro-aggregates are known to consist of both micro-aggregates and silt-clay sized aggregates (<53 μm) as well as POM.

Adams et al. (2011) argued that it is essential to model SOM dynamics more deterministically in order to reproduce the processes of physical protection. The conceptual model suggested by many authors in the scientific literature, that macro-aggregates are formed around particulate organic matter (POM), followed by the release of micro-aggregates as the occluded organic materials are decomposed (Golchin 1994; Balesdent et al., 2000; Puget et al., 2000; Plante and McGill, 2002; Six et al., 2002a; Six et al., 2002b; Six et al., 2004; Bronick and Lal, 2005, Helfrich et al., 2008; Nikolaidis and Bidoglio, 2011) has not been modeled yet. Significant improvement of carbon modelling will entail a deterministic explanation of the saturation capacity of the different carbon pools, estimation of the rates of occlusion or release of labile organic materials and therefore their availability for mineralization or stabilization (Plante and McGill, 2002), evaluation of soil structure (related with soil hydraulics and fertility) and optimization of the appropriate measures/practices to manage land use changes, and climate change (Bronick and Lal, 2005; Rees et al., 2005).

In this work a soil carbon, aggregation, and structure turnover (CAST) model and a simplified mechanistic N model were developed, based on current knowledge of the proposed mechanism in the relative scientific literature that suggests that macro-aggregates are formed around POM, followed by the release of micro-aggregates. The model was evaluated using field data of cropland to set aside conversions in a fine

textured Mediterranean site in Greece and a coarse textured humid continental site in Iowa.

2. Methodology

2.1. Model conceptualization and description

A schematic overview of current knowledge on macro-aggregate formation and destruction is provided in Figure 1. Plant residue is incorporated in the soil system and is colonized by microbial decomposers. Fungal hyphae, microbial metabolites and root exudates provide the binding for soil particles and smaller aggregates to cells of bacteria or fungi and form macro-aggregates around POM. Macro-aggregated POM is further decomposed and fragmented into smaller particles. Some of this finely fragmented POM becomes encrusted with mineral particles (silt-clay sized micro-aggregates) and microbial byproducts, leading to the formation of micro-aggregates within macro-aggregates. Biodegradation of the easily decomposable incorporated OM, results in the decrease of the microbial growth/activity and the supply of microbial biopolymers and macro-aggregates become less stable. Then if slaking occurs with rapid contact of aggregates with water these macro-aggregates would release stabilized micro-aggregates and silt –clay sized aggregates and highly decomposed residual POM would become unprotected. These materials may subsequently be reincorporated into new aggregates if fresh plant residue enters the system.

The structure of the developed soil carbon, aggregation, and structure turnover (CAST) model is depicted in Figure 2. The model was developed in MATLAB

(Version 7.10.0499 (R2010a). Three aggregate types are considered consisting of the relative RothC carbon pools with distinct turnover rates (Figure 2): Decomposable Plant Material (DPM), Resistant Plant Material (RPM), Microbial Biomass (BIO), Humified Organic Matter (HUM) and Inert Organic Matter (IOM). AC1, AC2, and AC3 are the three types of aggregate sizes incorporated in the model. The AC1 aggregate type corresponds to silt-clay sized aggregates (<53 μm), consisting of BIO, HUM, and IOM. The AC2 aggregate type corresponds to micro-aggregates (53–250 μm) consisting of BIO, HUM, IOM, and fine DPM and RPM pools. The AC3 aggregate type corresponds to macro-aggregates (>250 μm) consisting of BIO, HUM, IOM, and fine and coarse deriving DPM and RPM pools. Each carbon pool of the aggregate types decomposes by a first-order process with its own characteristic rate, in the same way as in RothC producing CO2, BIO and HUM, apart from the IOM pool which corresponds to biochar and is resistant to decomposition. The decomposition rate constant (k) is corrected by the product (abc) of three correction factors for the major factors determine microbial activity ('a' for temperature, 'b' for water deficit and 'c' for soil cover) as in RothC. The proportion that goes to CO2 and to BIO and HUM is determined by the clay content of the soil (Coleman and Jenkinson, 1999). The remaining C that is not lost is split into 46% BIO and 54% HUM, which are the default values for microbial efficiency used in RothC. In each time step, each organic compound is considered to decompose once; i.e. decomposition of each pool will follow fragmentation and aggregation after the updating of the pool mass.

The calculations of the processes represented in Figure 2 are presented in the following descriptive mass balance equations followed by detailed justification of the conceptual and model description.

2.1.1. Plant litter input apportionment and fragmentation

Plant material is considered to consist of the organic materials with different resistance to decomposition; progressively resistant carbohydrates and proteins, cellulose, hemicelluloses, and lignin (Van Veen and Paul, 1981). The model apportions plant litter input between Decomposable Plant Material (DPM), i.e. easily decomposable carbohydrates (i.e. O-alkyl C) and Resistant Plant Material (RPM), like recalcitrant

long chained C (i.e. alkyl C) (Golchin et al., 1994) using the factors reported by Coleman and Jenkinson (1999); i.e. 1.44 for grassland and 0.67 for shrub land. The DPM carbon pool is assumed to consist of coarse POM (53-250 μm), due to its very small turnover time and it is immediately available for aggregation. The RPM pool is fragmented due to earthworms, nematodes and other small fauna to coarse POM (>250 μm) (RPMc) and only its fragmented portion is available for aggregation. The fragmentation is described by first order kinetics. The two rate constants of fragmentation are corrected with the same 'abc' correction factors used for decomposition assuming that fragmentation will follow the same pattern. The RPM pool is the only pool of the fresh plant material that is not aggregated.

2.1.2. Macro-aggregate formation

Fresh plant material is rapidly colonized by microbial decomposers when it enters the soil matrix. Fungal hyphae mechanically bind the soil particles that surround the organic resource (Helfrich et al., 2008). Root mucilages as well as microbial mucilages released, like extracellular polysaccharides provide the glueing that bind them to cells of bacteria or fungi and form macro-aggregates around POM. Enough young POM is considered to have been incorporated for stable aggregates to be created (Puget et al., 2000). Macro-aggregation is therefore induced by the plant input and especially the DPM. It was considered that aggregation will take place when available plant material exists with favourable conditions for microbial activity (soil moisture and temperature), following first order kinetics at the same manner as decomposition (Equations 1-2). No aggregates will be formed if there is no DPM material. Coarse DPM and RPM is aggregated with AC1 and AC2 aggregates. It was assumed that

aggregates of constant composition (coarse plant material, AC1, and AC2) will be created depending on the rate of aggregation, the availability of plant material and the availability of AC1 and AC2. If neither AC1 nor AC2 is the limiting factor equations 3-6 are used for the calculations. As there is no evidence if macro-aggregation can take place even if AC1 or AC2 is not available it was assumed that both of them are limiting factors. Therefore, for example if AC2 is the limiting factor, Equations 7-9 are used ("carbon-limited" conditions).

Equations 1
Equations 2
Equations 3

Equations 4

Equations 5
Equations 6
Equations 7

Equations 8
Equations 9

The relative contribution of the pools within AC1 (BIO and HUM) and AC2 (BIO, HUM, fDPM, and fRPM) which are aggregated is determined proportional to the composition of the aggregates in these pools at this time step. For example in the case of AC1 Equations 10 and 11 are used.

Equations 10
Equations 11

The free coarse POM and AC1 and AC2 carbon pools are updated due to macro-aggregation. *Fragmentation of coarse POM in AC3:* As the intra-aggregate coarse

DPM and RPM POM decomposed are further fragmented with first order kinetics into smaller particles, finely fragmented POM (fPOM), and the microbial exudates are released, the macro-aggregates become more stable.

2.1.3. Micro-aggregate formation

Some of this fine plant material becomes encrusted with mineral particles and microbial byproducts (AC1 silt-clay sized micro-aggregates within AC3), leading to the formation of micro-aggregates within macro-aggregates (AC2 in AC3) and consequently an increased physical protection of the POM (Six et al., 2002a, Six et al., 2004). It was assumed that micro-aggregation also follows first order kinetics and that micro-aggregates of constant composition (fine plant material and AC1) will be created depending on the rate of aggregation, the availability of plant material and the availability of AC1, which is also a limiting factor. The existence of labile POM material (DPM) is not considered a limiting factor for micro-aggregation, since turnover times of micro-aggregates is order of magnitudes higher than the turnover time of decomposable plant materials. The composition of AC1 (BIO and HUM) aggregated is determined proportional to the composition of the pools at this time step (similarly with equations 10 and 11). The fine POM as well as AC1 in AC3 carbon pools are updated due to micro-aggregation.

2.1.4. Decomposition of carbon pools

The physical protection exerted by macro- and/or micro-aggregates on POM C is attributed to (Six et al., 2002a): (1) the compartmentalization of substrate and microbial biomass, (2) the reduced diffusion of oxygen into macro-aggregates and especially micro-aggregates which leads to a reduced activity within the aggregates, and (3) the compartmentalization of microbial biomass and microbial grazers. Grazing pressure on bacteria by bacterivorous nematodes for example is greater in sandy soils than in loams and clays resulting in a higher N mineralization rate per bacterium (Hassink et al., 1993). The compartmentalization between substrate and microbes by macro- and micro-aggregates is indicated by the highest abundance of microbes on the outer part of the aggregates and a substantial part of SOM being at the center of the aggregates (Golchin et al., 1994). The inaccessibility of substrate for microbes within aggregates is due to pore size exclusion and related to the water-filled porosity. The reduced diffusion of oxygen into macro-aggregates has been verified by increasing N2O fluxes observed with increasing water stable aggregate sizes, due to the existence of hot spots of anaerobiosis (Six et al., 2002a). Most of the decomposition products (BIO and HUM) of each pool in the AC3 and AC2 aggregates is assumed to contribute to the aggregate in which it is contained and only a small percent is leaked out in the free AC1 pool, since microorganisms and their immediate products of decay are considered to form a tightly closed system (Van Veen and Kuikman, 1990) (Figure 2, notice grey arrows indicate the respective fluxes). Specifically, it was assumed that 95% of the products produced by the decomposition of the coarse and fine DPM and RPM in the AC3 aggregate remain in the aggregate and are added in the AC1 within the AC3, while 5% is transferred in the free AC1 aggregate. Similarly, 95% of the products produced by the decomposition of the pools (BIO, HUM, fDPM, and fRPM) contained in the micro-aggregates within the macro-aggregates (AC2 in AC3) remain

in the micro-aggregates and half of the rest are added in the AC1 within the AC3, while the other half is transferred in the free AC3 aggregate. Likewise, 95% of the products produced by the decomposition of the free macro-aggregates (AC2) remain in the micro-aggregates and the rest 5% is transferred in the free AC1 aggregate. The decomposition products of the free AC1 as well the AC1 aggregate inside the macro-aggregates remain in the same pool. The carbon pools of the fresh organic matter (DPM, RPM and RPMc) decompose and the decomposition products (BIO and HUM) are transferred in the free AC1 aggregate.

2.1.5. Macro-aggregate destruction

Conceptually, further decomposition of the incorporated OM (utilization of the more labile pool, like the more easily decomposable carbohydrates), results in the decrease of the microbial growth/activity and the supply of microbial biopolymers and macro-aggregates become less stable. Then if slaking occurs with rapid contact of aggregates with water these macro-aggregates would release stabilized micro-aggregates and silt – clay sized aggregates and highly decomposed residual POM would become unprotected. It was assumed that the consumption of the glue (microbial metabolites) which cause the macro-aggregate destruction would be positively correlated with the availability of the DPM pools. New aggregates will be formed in a system where permanent flow of decomposable material is introduced if there is availability of free AC1 and AC2.However, older aggregates will deterioriate and eventually be destroyed. Therefore, it was introduced a pseudo percent value for the fine and coarse DPM pools content of the AC3 aggregate, below which macro-aggregates are considered unstable and therefore ‘potentially’ destroyed. Macro-aggregate destruction

is determined by the concentration of the labile pool of the particulate organic matter (DPM pools). In the field, water unstable macro-aggregates will be destructed if slaking occurs in relation with the precipitation and irrigation events. Destruction due to tillage has not been introduced at this point in the model. The pools of the free plant material and the free AC1 and AC2 are updated after the destruction of the macro-aggregates and the final calculations are made. These materials may subsequently be reincorporated into new aggregates if fresh plant residue is introduced in the system.

2.1.6. Soil bulk density and porosity sub-model

Porosity was calculated according to the equation: porosity (%) = (Ds−Db)/Ds, where Ds is the soil particle density, and Db the soil bulk density. Ds is calculated according to Adams (1973): Ds=100 / (OM%/Dom + (100-OM%)/Dm), where Dom is the organic matter particle density and Dm, the particle density of the mineral phase. Dom and Dm were calibrated so as to obtain the field measurements. OM% is the soil organic matter content in g/100 g soil which is calculated by multiplying the SOC content with the factor 1.724. Soil bulk density is calculated by dividing the soil mass with the apparent volume of the aggregates. In order to estimate the apparent volume of the aggregates, the bulk density of the aggregates is calculated first. It was considered in accordance with Malamoud et al. (2008) that aggregates are regarded as spheres with different packing systems to explain the differences in bulk density (Equations 12-14). Aggregate type 1 is the less porous whereas the type 3 is the less dense.

Aggregate type 1: pyramidal system, — Equation 12

Aggregate type 2: tetragonal sphenoidal, — Equation 13

Aggregate type 3: simple cubic, – Equation 14

Ds of each aggregate is calculated again according to Adams (1973). The OM% of each aggregate is taken by the equation OMx=ACx*1.724*100/mass_ACx. However, the bulk density of the mineral phase for each aggregate is assumed to be the same in this modelling exercise, although it would be by definition vary, being higher in smaller aggregates. Then the apparent volume of each aggregate type is calculated via: Vx = mass_ACx /BDx. Soil mass changes as OM content changes. In order to estimate the mass of the three aggregate types, it was assumed that carbon transfer related with aggregation and disruption can be related with silt-clay transfers, whereas only clay mass was assumed from Malamoud et al., (2008) under a different conceptualization, where transfers were not calculated. Silt-clay mass transfer is determined by its concentration as Carbon and the carbon transfer calculated by macro-aggregation, micro-aggregation, and disruption in every time step (equation 15, an example of Silt-clay mass transfer for macro-aggregation). A correction factor (cf) to adjust for non linearities is introduced in each aggregate. Silt-clay related carbon is considered the BIO and HUM pools (equation 16). The mass of the aggregates is then calculated according to equations 17-19. The fractions that determine the distribution of sand mass in each aggregate type (f1 and f2) are estimated by the field measurements.

Equation 15

Equation 16
Equation 17
Equation 18
Equation 19

2.1.7. Mechanistic estimation of N stocks

Finally, a simplified mechanistic model was developed for the estimation of the N stocks of the organic matter pools of the CAST model. N stocks for each 'x' pool were calculated according to the equation: $N_x=C_x/(C/N)_x$, where Cx is the respective calibrated value derived by the CAST model. The C-to-N ratio of each pool is then calibrated to meet the field measured N stocks. The optimization was constrained by the following conditions: $4<(C/N)_x<50$, $4<(C/N)_{BIOx}<14$, and $(C/N)_{RPM\ \&\ RPMc}>(C/N)_{DPMc}$, for the free POM pools. An optimization routine in excel, the 'solver' (Microsoft office excel, 2007) was used for the optimization procedure.

2.2. Field data used for model evaluation

Data from Koiliaris River Basin and Clear Creek Basin, Critical Zone Observatories (www.soiltrec.eu) were used to evaluate the model. The sites correspond to crop production to set aside conversions and have been already modeled with RothC carbon model (Stamati et al., 2012). The two sites are described in detail by Stamati et al. (2012). The first site (indicated as IA) was Iowa City, IA, USA (41°45´N, 91°44´W, 230 m), indicative of humid continental climate with soils of coarse texture-sandy loam (clay=7%). The second site (indicated as GR) was in the northern part of Chania Prefecture, Crete, Greece (39°25´N, 51°41´E, 10 m), where typical semi-arid, Mediterranean climate dominates with soils of finer texture-clay loam (clay=30%). Topsoil (10 cm) samples were analyzed for water stable aggregates (Elliott 1986); macro-aggregates (>250 μm), ii) micro-aggregates (53-250 μm), and iii) silt-clay sized micro-aggregates and minerals (<53 μm). Macro-aggregates were separated, according to the procedure described by Lichter et al., (2008) into the following fractions: i) coarse particulate organic matter and sand (cPOM: >250 μm), ii) easily dispersed silt-

clay fractions (sc-M <53 μm), and iii) micro-aggregates (mM: 53-250 μm). The mM fraction was further separated to fine particulate organic matter and sand (fPOM: 53-250 μm) and silt-clay fraction of the micro-aggregate (sc-mM <53 μm). Similarly, micro-aggregates (53-250 μm) were separated to fine particulate organic matter (fPOM: 53-250 μm) and the silt-clay fraction (sc-mM <53 μm) they contained. The C and N distributions in the isolated carbon pools as well the silt-clay mass of the aggregate fractions and its concentration in carbon (Table 1a and 1b) were used for the initialization and calibration of the model

2.3. Methodology for initialization and calibration of the model

The following assumptions were made in order to initialize the model. Litter carbon pools (DPM, RPM, RPMc) were assumed to be zero. The fine POM contained in free micro-aggregates and micro-aggregates within the macro-aggregates were equally apportioned to DPM and RPM. The fine POM, both DPM and RPM, in the macro-aggregates not occluded in micro-aggregates, was considered zero. The coarse POM contained in the macro-aggregates was primarily attributed to RPM and a small fraction to DPM. Biomass was considered to be the 5% of the related silt-clay sized carbon pool. The biochar (IOM), since there were not available field measurements in the modelling exercise, was considered to be zero. The percent of the decomposition products (BIO and HUM) of each pool which contribute to the aggregate it is contained in, and the percent that is leaked out in the free AC1 pool, as discussed above, and were not calibrated; values of 95% and 5% were set arbitrarily. Since the two sites had been calibrated before with the RothC model (Stamati et al., 2012), the calibrated plant litter input (3.79 t C/ha and 5.05 t C/ha in Greece and Iowa,

respectively) was introduced in the model and the estimated decomposition rate constants were used as initial values for the calibration procedure. The decomposition rate constants were calibrated by testing proportionally higher values for the unprotected and less protected pools and proportionally lower for the most protected pools, assuming that decomposition occurs at a slower rate within macro-aggregates as compared with non-aggregate-associated POM due to diffusion limitation of O_2(g).

3. Results and discussion

The CAST model was able to capture the SOC content as well the carbon content of the three aggregate types in both Greek and Iowa sites (Figure 3Aa and 3Ba). The carbon content of the aggregate type 3 (AC3) plus the coarse particulate organic matter of the non aggregated pools (cPOM) is compared with the field measured carbon content of the macro-aggregates (Figure 3Ab and 3Bb). Similarly, the composition of the AC3 in silt-clay sized aggregates (AC1 in AC3) and micro-aggregates (AC2 in AC3) was calibrated. The fine particulate organic matter of the micro-aggregates (fPOM AC2inAC3) plus the intra macro-aggregated fPOM (fPOM inAC3) was compared with the respective field measured fPOM.

The calibrated values of the rate constants and turnover times of the carbon, aggregate and structure turnover model for the Greek and the Iowa cropland to set aside conversion are presented in Table 2. The monthly correction factors ‘abc’ for rate constants are presented in Table 3. Litter fragmentation to coarse POM exhibited turnover times of 0.12 and 0.18 years in Greece and Iowa respectively. Litter fragmentation due to earthworms, nematodes and other small fauna seem to be

facilitated in the coarser texture of the Iowa site. The turnover time of fragmentation of the coarse macro-aggregated POM was similar in both sites for the DPM pool 3.5 years (Greece) and 3.6 years (Iowa). On the contrary, the RPM pool turnover time (fragmentation) was almost 4 times higher in Greece (17.7 years) as compared with Iowa (4.6 years). This pattern could be attributed to different quality composition of the RPM material (shrub land in Greece versus grassland in Iowa), while the composition of the DPM materials seem to be similar in both sites.

The turnover time in years (1/annual decomposition rate) was estimated to be for the litter and non-aggregated resistant to decomposition POM 5.8 and 7.3 years for the Greek and Iowa site respectively, while macro-aggregation resulted in doubling the protection (11.8 years) in Greece while it was 1.4 times higher in Iowa (10.4 years). The coarse POM has been found to be the primary source of mineral N in topsoil (Zeller and Dambrine, 2011). Its C/N ratio is negatively related with mineralization due to immobilization. Potential mineralizable N, potential soluble organic N and C, as well carbohydrate C increased in the set-aside soils by a factor of 4.9, 3.5, 2.9, and 2.7 for Iowa and only 1-1.5 times for Greece (Stamati et al., 2012). The more increase observed in the case of Iowa may be can be related with the quality of the litter (grassland versus shrub land). Moreover, the seasonal pattern of decomposition due to climatic conditions may also play a role (Figure 4).

More protected was the respective fine POM in micro-aggregates within the macro-aggregates; a 40% more protection as compared with the macro-aggregated cPOM was estimated (16.5 and 14.6 years, for the Greek and Iowa site, respectively). The fine RPM of the free micro-aggregates presented turnover times (8.5 and 9.4 and 14.6 years, for the Greek and Iowa site, respectively) lower than both the fine and coarse

RPM related with macro-aggregates, but higher than the non-aggregated RPM carbon pools. On the other hand the coarse decomposable plant material presented more than 3 times higher turnover due to macro-aggregation (0.6 and 1.2 years, for the Greek and Iowa site, respectively) as compared with the non-aggregated coarse DPM (0.2 and 0.4 years, for the Greek and Iowa site, respectively). The fine DPM of both macro and micro aggregates (1.2 and 2.4 years, for the Greek and Iowa site, respectively) exhibited 2 times higher turnover compared to the relative coarse macro-aggregated POM. The turnover time of the silt-clay related carbon (humus) of the micro-aggregates within macro-aggregates (841.8 and 72.9 years, for the Greek and Iowa site, respectively) was 1.5 and 3.8 times, for the Greek and Iowa site, higher than the silt-clay sized aggregates within macro-aggregates (570.3 and 19.2 years, for the Greek and Iowa site, respectively). Whereas, the turnover time of the micro-aggregates (AC2) and silt-clay sized aggregates (AC1) was lower (346.6 for the Greek and 12.2 and 8.1 years for the Iowa site, respectively). Finally, the calibrated turnover of the biomass carbon pools was the same in all fractions and estimated to be 2.9 years in the Greek site and 5.5 years in the Iowa site.

Overall, the decomposition rates were found to be significantly higher in the Iowa site as compared with the Greek, which can be attributed primarily to the climatic conditions and the soil texture of the two sites. The high decay constant of the HUM pools (silt-clay associated carbon) in the Iowa site as it was suggested by the results of Stamati et al. (2012) is attributed to the very low clay content in accordance with Balesdent et al. (1998) and Gottschalk et al. (2010). They showed that SOC in the size fraction <50 μm is made up of the relatively rapidly decomposing pool of silt associated C (decay constant of 0.12 y^{-1}), and a relatively slowly decomposing pool of clay associated C (decay constant of 0.03 y^{-1}), Nevertheless, the wet and warm

summers in Iowa hasten organic matter decomposition. On the other hand, the significantly low HUM decomposition rates in Greece have been attributed to slaking of the soil surface due to high clay content which can result in fine soil particles moving into inter-aggregate pores in the surface area, which can reduce the infiltration rate of rainfall or irrigation water and reduce hydraulic conductivity. Presence of biochar could be another possible explanation.

The turnover time for macro-aggregation under no limiting factor was found to be a few years (Puget et al., 2000), 2.9 years in Greece and 5.6 years in Iowa. Similarly the micro-aggregation inside the macro-aggregates exhibited turnover time of 8.8 and 12.2 years respectively. The formed macro-aggregates contained 30% carbon related with the AC1 and 30% carbon related with the AC2, in the case of the Greek site. In Iowa, the formed macro-aggregates contained 35% carbon related with the AC1 and 5% carbon related with the AC2. The formed micro-aggregates inside the macro-aggregates exhibited 23.4 and 18% fine POM content, in Greece and Iowa, respectively. The soil system reaches a maximum macro-aggregation after about 7 years in the Greek site and 14 years in the Iowa site (Figure 3). Jastrow et al. (1996) also found that macro-aggregation reached a maximum after 10.5 complete growing seasons since cultivation (prairie restorations). In both sites, the limiting factor for macro-aggregation is the availability of AC1. The sum of the carbon related with the AC3 and the free coarse POM is stabilized to a steady-state carbon content. Macro-aggregate disruption is taking place after this period from January to April in Greece and from August to December in Iowa, presenting a constant seasonal pattern, in accordance with Plante et al. (2002) and Six et al. (2004) who suggested that, macro-aggregation in agroecosystems shows seasonal dynamic. Total SOC after this period increases due to the increase of micro-aggregates (AC2), indicating that maximum

physical protection capacity for SOM is determined by the maximum micro-aggregation, which is in turn, determined by clay content and type, in accordance with Six et al., (2002a) suggestions. Macro-aggregate destruction takes place when macro-aggregates contain lower than 0.15% and 1% DPM in the Greek and Iowa site, correspondingly.

The simulated evolution of silt-clay mass and carbon content (%) of the silt-clay fraction, related to aggregate type 1 (AC1), type 2 (AC2), silt-clay sized aggregates within in the type 3 (AC1 in AC3), and micro-aggregates within the type 3 (AC2 in AC3) are presented in Figure 5. The calibrated values of the particle density of the organic matter (DOM) an the mineral phase were found to be 2.2 and 0.7 g cm^{-3} in Greece and 1.9 and 0.5 g cm^{-3} in Iowa. Lower density of the mineral phase in Iowa is in accordance with the coarser texture. The lower density of the organic matter can be possible explained by the different litter quality and would be expected to be lower in grassland (Iowa) compared to shrub land (Greece) due to lower lignin content. The 46% of the sand mass in the Greek site was found to be in the free micro-aggregates (AC2) and the rest 54% in the macro-aggregates (AC3). Coarser sand was found in the Iowa site, where 29% was related with the micro-aggregates (AC2) and 71% with the macro-aggregates (AC3).

The correction factors to adjust for non linearities for silt-clay flow related with macro-aggregation and micro-aggregation inside the macro-aggregates where found to be in the Greek site 0.8, 2.2 and 0.16 for the AC1, AC2 and AC1 in AC3, respectively. Similarly, for the Iowa site they were 0.8, 2.0, and 0.5. A value close to 1 means that silt-clay mass flow is linearly related to OC flow. The significantly higher than 1 value support the recent imaging and X-ray spectroscopic work (see Review of Kleber and

Johnson, 2010) which suggest that substantial parts of mineral surfaces are not covered by organic matter and differentiate from the mineral sorbent—organic sorbate idea. Finally, the significantly lower than 1 values, possible indicate hot-spots of high OC concentration, where the micro-aggregation is induced. With this approach the prediction of the OC (%) content of the different silt-clay fractions was achieved. When the soil system is at the maximum macro-aggregation in both sites (7^{th} year in Greece and 14^{th} year in Iowa), the silt-clay mass of the AC1 and AC2 is at minimum and the OC (%) content of these pools reaches a maximum. In both sites, the limiting factor for macro-aggregation is the availability of AC1. In both sites the porosity and bulk density reach a maximum and minimum, respectively, when the soil system is at the maximum macro-aggregation and then due to the increase of micro-aggregates bulk density increases and porosity decreases towards to a stable value, both presenting however an inter-annual variability (Figure 6).

SOM stabilization efficiency was reduced after the soil system reached maximum aggregation (Figures 3 and 4). Plante and McGill (2002) and Six et al. (2004) have also suggested that in native systems, at the maximum aggregate level lower amount newly incoming fresh residuean is stabilized in accordance with the results presented in Figure 3a. An intermediate aggregate turnover is optimum in order to have aggregate formation and occlusion and subsequent protection of C (highest sequestration rate). Kimetu et al. (2009) also indicated that SOM stabilization efficiency was highest with intermediate cultivation history of about 20 years as compared with both degraded soils and high C-containing soils due to limited protection of organic matter by minerals. The reduced efficiency was less pronounced in the Greek site as compared with the Iowa site due to the higher amount of clay.

The C-to-N ratio of the OM pools after the calibration of the mechanistic N model for the Greek and the Iowa cropland to set aside conversion are given in Table 4. The simulated evolution of the C-to-N ratio of soil, AC1, AC2, and AC3 plus the non-aggregated cPOM are presented in Figure 7. In the Iowa site the model was able to capture the variation of C-to-N ratio in all aggregate pools. The C-to-N ratio in soil, AC2, and AC3 plus the non-aggregated cPOM increased to a maximum value similarly with macro-aggregation and porosity maximum and bulk density minimum, and then decrease to a stable value. On the contrary, the C-to-N ratio of the AC1 aggregate type decreased to a stable value. In the Greek site, the optimum solution could not represent the field variation of the C-to-N ratio of the AC1 aggregate. The C-to-N ratio of soil, AC2, and AC3 plus the non-aggregated cPOM seem to increase towards a stable value. The C-to-N ratio of the biomass pools was found to be, in general higher in the Iowa site (10.5 to 14) as compared with Greek site (4.3 to 14), indicating possible more abundance of fungi populations. The biomass found in the macro-aggregates exhibited higher C-to-N ratio compared to the biomass related to the AC1 and AC2 aggregates in Iowa, indicating in this way a possible relation of fungi presence with macro-aggregation in the coarse textured Iowa site. Conversely, in the Greek site higher C-to-N ratio (coinciding with the introduced upper limit constraint) was observed in the biomass pools related to AC1 and AC1 in AC3, in comparison with the biomass pools related to AC2 and AC2 in AC3, where values which indicate bacteria predominance were found (6.7 and 4.3 respectively). The C-to-N ratio of the HUM pools in the Iowa site was lower than in the Greek site. In the Iowa site the ratio ranged from 10 to 13.5 being lowest in the HUM pool of the AC2 in AC3. In the Greek site the respective ratio ranged from 7.3 to 30.1, being highest in the HUM pool of the AC2 in AC3. The C-to-N ratio of the litter and non aggregated POM pools was

higher in the Iowa site compared to the Greek site, whereas the aggregated POM pools exhibited higher C-to-N ratio in the Greek site as compared with the Iowa site, apart from two exceptions (DPM fine POM in AC2 and DPM fine POM in AC3). The DPM pools showed higher C-to-N ratio compared to the RPM pools in both sites, apart from the DPM and POM pools in micro-aggregates within the macro-aggregates (AC2 in AC3), where the opposite pattern was observed.

4. Conclusions

This work constitutes the first attempt to model the conceptual macro-aggregate formation around particulate organic matter and subsequent release of micro-aggregates due to macro-aggregate turnover. Soil carbon pools as described by the RothC model were coupled with aggregate and structure turnover modules and validated with field data from two sites. The developed CAST model was successfully used for the simulation of carbon, aggregate, and structure turnover in cropland to set aside conversions in Greece (fine textured Mediterranean) and Iowa (coarse textured humid continental).

- The model was able to capture the carbon content and the C-to-N ratio content of the pools comprising the three aggregate types (macro-aggregates: >250 μm, micro-aggregates: 53-250 μm, silt-clay sized aggregates: <53 μm) in both sites.
- A more deterministic explanation of the saturation level of the different carbon pools and soil structure (porosity and bulk density) were obtained. The soil system reached maximum macro-aggregation/porosity and minimum bulk density after 7 and 14 years in Greece and Iowa, respectively. Afterwards, macro-aggregate

disruption presented a constant seasonal pattern and any further SOC increase was due to micro-aggregation resulting in the increase of bulk density and decrease of porosity towards to a stable value.

- The module for the calculation of the silt-clay fractions mass flow between the aggregates and their carbon concentration supported recent scientific findings that suggest that substantial parts of mineral surfaces are not covered by organic matter and differentiate from the mineral sorbent—organic sorbate idea (Kleber and Johnson, 2010).
- The developed simple mechanistic Nitrogen model suggested plausible differences in the C-to-N ratio of the biomass pools between the two sites (i.e. abundance of fungi populations in the coarser textured Iowa site or fungi presence within the macro-aggregate fraction).

The CAST model can assist in revealing primary factors determine organic matter, aggregation, and structure turnover in different ecosystems. This capability should allow better prediction of the response of the soil system to management practices, land use changes, and climate change in order to design and optimize the appropriate measures/practices.

Acknowledgements

The authors acknowledge funding support from the European Commission FP 7 Collaborative Project *Soil Transformations in European Catchments (SoilTrEC)* (Grant Agreement No. 244118). F.E. Stamati was supported by a Ph.D. fellowship from Bodosaki Foundation. We would like also to thank the authors of STRU-C model (Malamoud et al., 2008) for kindly providing their source code.

References

Baldock, J.A. (2007). Composition and cycling of organic carbon in soils. P. Marschner, and et al (eds), Nutrient Cycling in Terrestrial Ecosystems, (Soil Biology; 10): 1-35.

Balesdent, J., Besnard, E., Arrouays D., Chenu, C., 1998. The dynamics of carbon in particle-size fractions of soil in a forest-cultivation sequence. Plant Soil 201, 49–57.

Balesdent, J., Chenu, C., and Balabane, M., 2000. Relationship of soil organic matter dynamics to physical protection and tillage. Soil and Tillage Research 53, 215–230.

Bechtold, J.S., and Naiman, R.J., 2009. A Quantitative Model of Soil Organic Matter Accumulation During Floodplain Primary Succession. Ecosystems 12, 1352–1368.

Bronick, C.J., Lal, R., 2005. Soil structure and management: a review. Geoderma 124, 3 –22.

Davidson, E. A., and Janssens, I. A. 2006. Temperature sensitivity of soil carbon decomposition and feedbacks to climate change. Nature 440, 165–173.

Falloon, P., and Smith, P., 2002. Simulating SOC changes in long term experiments with RothC and Century: model evaluation for a regional scale application. Soil Use and Management 18, 101-111.

Gleixner, G., Poirier, N., Bol, R., Balesdent, J., 2002. Molecular dynamics of organic matter in a cultivated soil. Organic Geochemistry 33, 357–366

Golchin, A., Oades, J.M., Skjemstad, J.O., and Clarke, P., 1994 Study of free and occluded particulate organic matter in soils by solid state 13C CP/MAS NMR spectroscopy and scanning electron microscopy. Australian Journal of Soil Research 32, 285–309.

Golchin, A., Clarke, P., Oades, J.M., Skjemstad, J.O., 1995. The effects of cultivation on the composition of organic matter and structural stability of soils. Australian Journal of Soil Research 33, 975–993.

Gottschalk, P., Bellarby, J., Chenu, C., Foereid, B., Smith, P., Wattenbach, M., Zingore, S., Smith, J., 2010. Simulation of soil organic carbon response at forest cultivation sequences using 13C measurements. Organic Geochemistry 41, 41–54.

Grandy A.S., Neff J.C., 2008. Molecular C dynamics downstream: The biochemical decomposition sequence and its impact on soil organic matter structure and function. Science of the Total Environment 404, 297-307.

Hassink, J., Bouwman, L.A., Zwart, K.B., Bloem, J., and Brussaard, L., 1993. Relationships between soil texture, physical protection of organic matter, soil biota, and C and N mineralization in grassland soils. Geoderma 57, 105-128.

Hassink, J., 1997. The capacity of soils to preserve organic C and N by their association with clay and silt particles. Plant Soil 191, 77–87.

Hassink, J., and Whitmore, A.P, 1997. A model of the physical protection of organic matter in soils. Soil Science Society of America Journal 61, 131–139.

Helfrich, M., Ludwig, B., Potthoff, M., Flessa, H., 2008. Effect of litter quality and soil fungi on macroaggregate dynamics and associated partitioning of litter carbon and nitrogen. Soil Biology and Biochemistry 40, 1823–1835.

Jastrow, J.D. 1996. Soil aggregate formation and the accrual of particulate and mineral-associated organic matter. Soil Biology and Biochemistry 28, 665-676.

Kleber, M., and Johnson, K.J., 2010. Advances in Understanding the Molecular Structure of Soil Organic Matter: Implications for Interactions in the Environment. Advances in Agronomy 106, 77-142.

Kleber M., Sollins P., Sutton R., 2007. A conceptual model of organo-mineral interactions in soils: self-assembly of organic molecular fragments into zonal structures on mineral surfaces. Biogeochemistry 85, 9–24.

Kimetu, J.M., Lehmann, J., Kinyangi, J.M., Cheng, C.H., Thies, J., Mugendi, D.N., Pell, A., 2009. Soil organic C stabilization and thresholds in C saturation. Soil Biology and Biochemistry 41, 2100–2104.

Knicker, H., 2007. How does fire affect the nature and stability of soil organic nitrogen and carbon? A review. Biogeochemistry 85, 91–118.

Malamoud, K., McBratney, A.B., Minasny, B., and field, D.J., 2009. Modelling how carbon affects soil structure. Geoderma 149, 19-26.

Molina, J.A.E., Clapp, C.E., Shaffer, M.J., Chichester, F.W., and Larson, W.E., 1983. NCSOIL, a model of nitrogen and carbon transformation in soil: description, calibration and behaviour. Soil Science Society of America Journal 47, 85-91.

Nikolaidis, N.P. and Bidoglio G., Modeling of Soil Organic Matter and Structure Dynamics: A Synthesis Review. Geoderma (submitted revisions).

Plante, A.F., McGill, W.B., 2002. Soil aggregate dynamics and the retention of organic matter in laboratory-incubated soil with differing simulated tillage frequencies. Soil and Tillage Research 66, 79–92.

Plante, A.F., Feng, Y., McGill, W.B., 2002. A modeling approach to quantifying soil macroaggregate dynamics. Canadian Journal of Soil Science 82, 181–190.

Porter, C.H., Jones, J.W., Adiku, S., Gijsman, A.J., Gargiulo, O., Naab J.B. Modeling organic carbon and carbon mediated soil processes in DSSAT v4.5, Operational Research 10(3), 247-278.

Powlson, D.S., Whitmore, A.P., Goulding, K.W.T., 2011. Soil carbon sequestration to mitigate climate change: a critical re-examination to identify the true and the false. European Journal of Soil Science 62, 42-55.

Puget, P., Chenu, C., and Balesdent, J., 2000. Dynamics of soil organic matter associated with particle-size fractions of water-stable aggregates. European Journal of Soil Science 51, 595-605.

Schoning, I., Morgentoth, G., Kogel-Knabner, I., 2005. O/N-alkyl and alkyl C are stabilised in fine particle size fractions of forest soils. Biogeochemistry 73, 475–497.

Six, J., Conant, R.T., Paul E.A., and Paustian, K., 2002a. Stabilization mechanisms of soil organic matter: Implications for C-saturation of soils. Plant and Soil 241, 155–176.

Six, J., Feller, C., Denef, K., Ogle, S.M., de Moraes, J.C., Alberecht, A., 2002b. Soil organic matter, biota and aggregation in temperate and tropical soils – Effects of no-tillage. Agronomie 22, 755–775.

Six, J., Bossuyt, H., Degryze, S., Denef, K., 2004, A history of research on the link between (micro)aggregates, soil biota, and soil organic matter dynamics. Soil and Tillage Research 79, 7–31.

Stamati, F.E., Nikolaidis, N.P., Schnoor, J.P., 2012. Modeling topsoil carbon sequestration in two contrasting crop production to set aside conversions with RothC-calibration issues and uncertainty analysis. Agriculture Ecosystem and Environment (in review).

Takeshi, I., and Moorcroft, P.R., 2006. The global-scale temperature and moisture dependencies of soil organic carbon decomposition: an analysis using a mechanistic decomposition model. Biogeochemistry 80, 217–231.

Van Veen, J.A., and Paul, E.A., 1981. Organic carbon dynamics in grasslands and soils. 1. Background information and computer simulation. Canadian Journal of Soil Science 61, 185-201.

Van Veen, J.A., and Kuikman,P.J., 1990. Soil structural aspects of decomposition of organic matter by micro-organisms Biogeochemistry 11, 213-233, 1990.

Virto, P., Barré, C., Chenu, 2008. Microaggregation and organic matter storage at the silt-size scale. Geoderma 146, 326–335.

von Lützow M., Kögel-Knabner I., Ekschmitt K., Flessa H., Guggenberger G., Matzner E., Marschner B., 2007. SOM fractionation methods: Relevance to functional pools and to stabilization mechanisms. Soil Biology and Biochemistry 39, 2183-2207.

Yang, X., Wang, M., Huang, Y., Wang, Y., 2002. A one-compartment model to study soil carbon decomposition rate at equilibrium situation. Ecological Modeling 151, 63–73.

Zeller, B., Dambrine, E., 2011. Coarse particulate organic matter is the primary source of mineral N in the topsoil of three beech forests. Soil Biology and Biochemistry 43, 542-550.

List of Figure Captions

Fig. 1. Schematic overview of macro-aggregation.

Fig. 2. Schematic representation of the carbon and aggregate turnover in the CAST model.

Fig. 3. Simulated evolution of carbon content of modeled pools in the A) Greek and the B) Iowa cropland to set aside conversion, a) soil (SOC), aggregate type 1 (AC1), type 2 (AC2), and type 3 (AC3) plus the coarse POM of the non aggregated pools (cPOM), b) the different pools contained in the aggregate type 3: silt-clay sized aggregates (AC1 in AC3), silt-clay related carbon of the micro-aggregates (silt-clay AC2inAC3), fine POM of the micro-aggregates (fPOM AC2inAC3) plus the intra macro-aggregated fPOM (fPOM inAC3), macro-aggregated cPOM (cPOM inAC3) plus the cPOM of the non aggregated pools. Points indicate the field measurements of the same colored line.

Fig. 4. Seasonal pattern of emissions of a) the coarse RPM litter pool and b) the soil (in the right up corner the small figure indicates the annual emissions for 20 years).

Fig. 5. Simulated evolution in the A) Greek and the B) Iowa cropland to set aside conversion of a) silt-clay mass and b) carbon content (%) of the silt-clay fraction, related to aggregate type 1 (AC1), type 2 (AC2), silt-clay sized aggregates within the type 3 (AC1 in AC3), and micro-aggregates within the type 3 (AC2 in AC3).

Fig. 6. Simulated evolution in the A) Greek and the B) Iowa cropland to set aside conversion of porosity (%) and bulk density (g/cm^3). Points indicate the field measurements of the same colored line.

Fig. 7. Simulated evolution of carbon-to-nitrogen ratio in the A) Greek and the B) Iowa cropland to set aside conversion, of soil, aggregate type 1 (AC1), aggregate type

2 (AC2), and aggregate type 3 (AC3) plus the coarse particulate organic matter of the non aggregated pools (cPOM). Points indicate the field measurements.

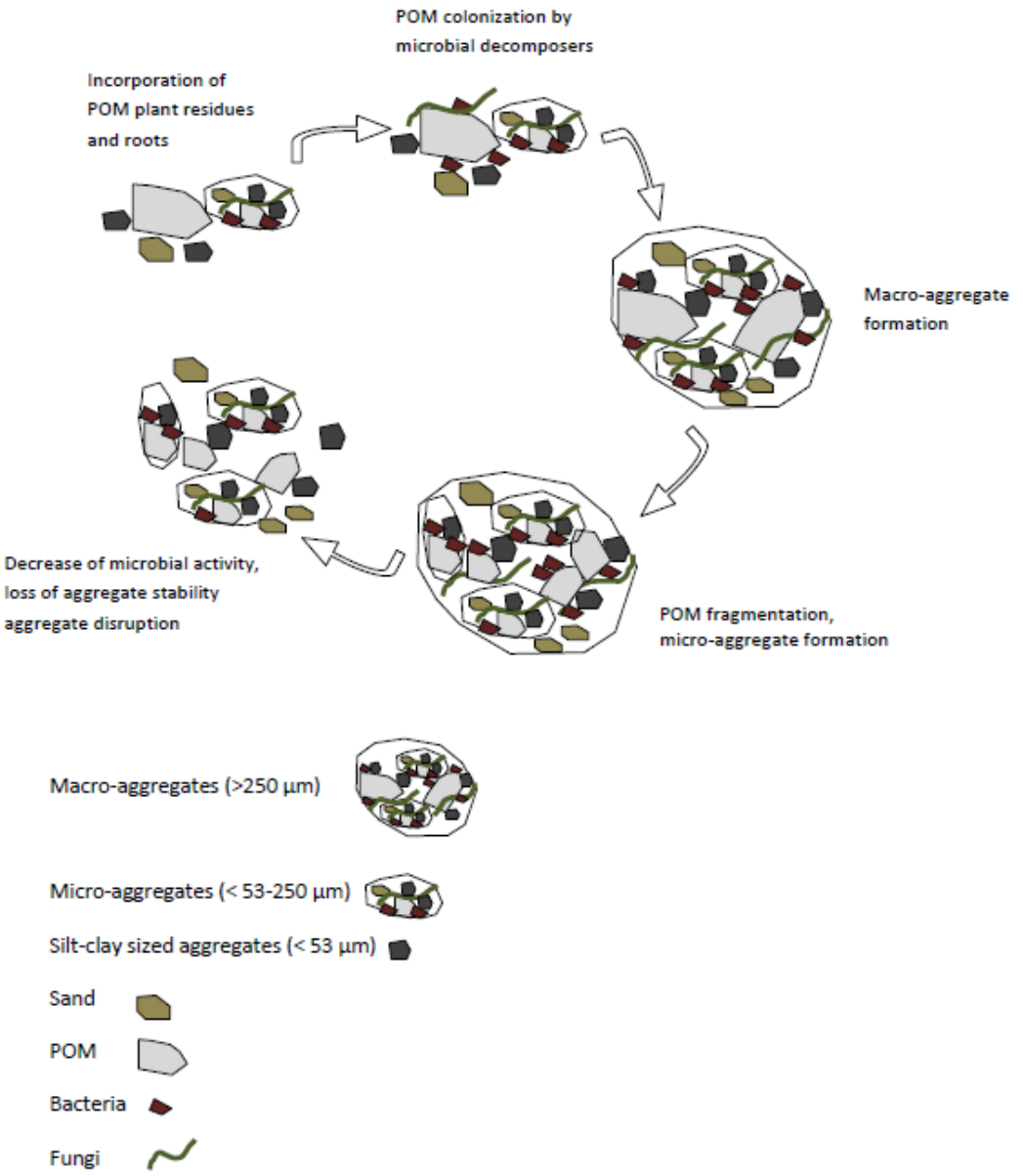
POM colonization by
microbial decomposers
Incorporation of
POM plant residues
and roots
Macro-aggregate
formation
POM fragmentation,
micro-aggregate formation
Decrease of microbial activity,
loss of aggregate stability
aggregate disruption
Macro-aggregates (>250 µm)
Micro-aggregates (< 53-250 µm)
Silt-clay sized aggregates (< 53 µm)
Sand
POM
Bacteria
Fungi

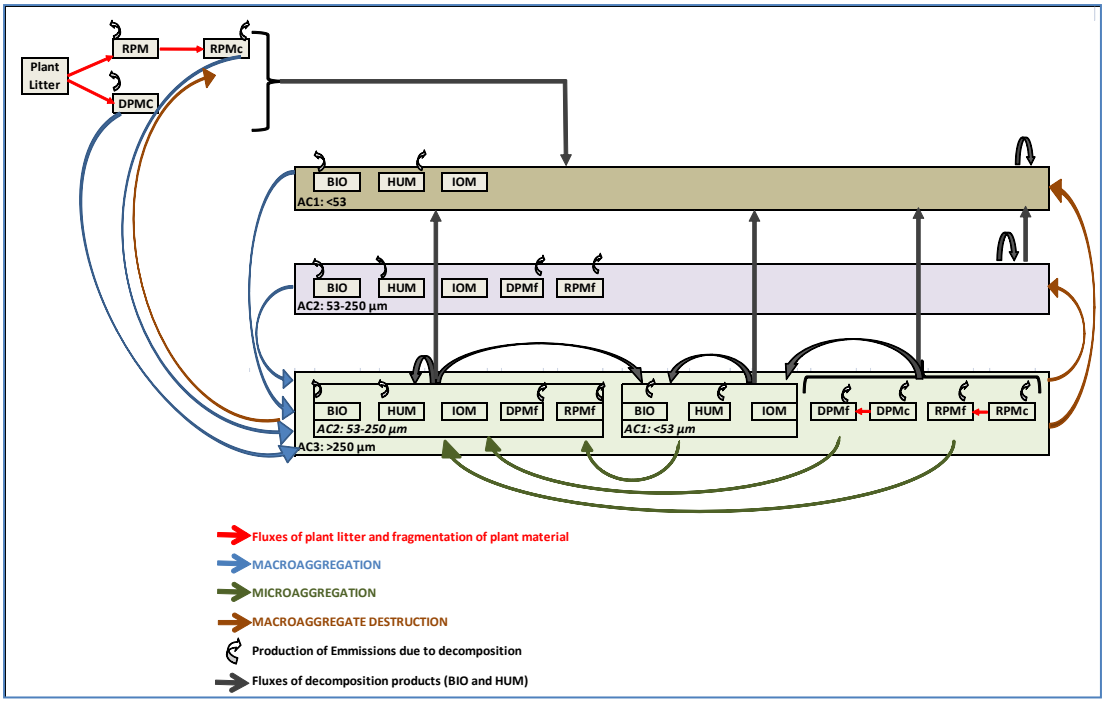
Plant Litter
RPM
RPMc
DPMC
BIO
HUM
IOM
AC1: <53
BIO
HUM
IOM
DPMf
RPMf
AC2: 53-250 µm
BIO
HUM
IOM
DPMf
RPMf
AC2: 53-250 µm
AC3: >250 µm
BIO
HUM
IOM
AC1: <53 µm
DPMf
DPMc
RPMf
RPMc
Fluxes of plant litter and fragmentation of plant material
MACROAGGREGATION
MICROAGGREGATION
MACROAGGREGATE DESTRUCTION
Production of Emmissions due to decomposition
Fluxes of decomposition products (BIO and HUM)

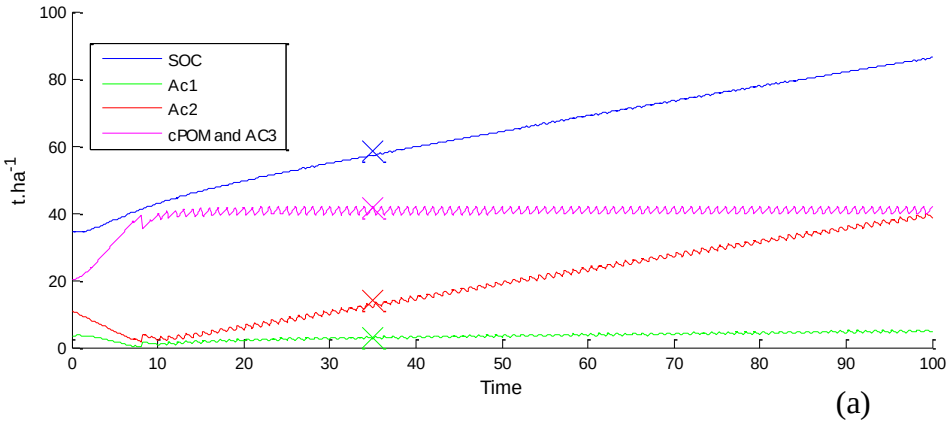
SOC
Ac1
Ac2
cPOM and AC3
t.ha-1
Time

(a)

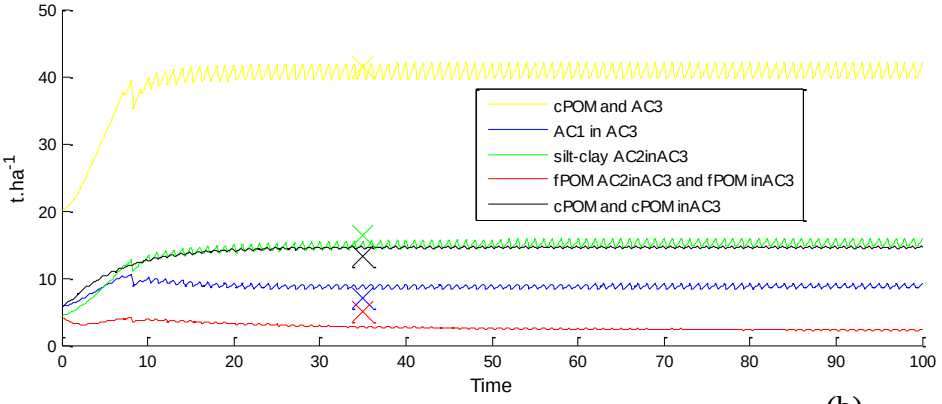
cPOM and AC3
AC1 in AC3
silt-clay AC2inAC3
fPOM AC2inAC3 and fPOM inAC3
cPOM and cPOM inAC3
t.ha-1
Time

(b) **(A)**

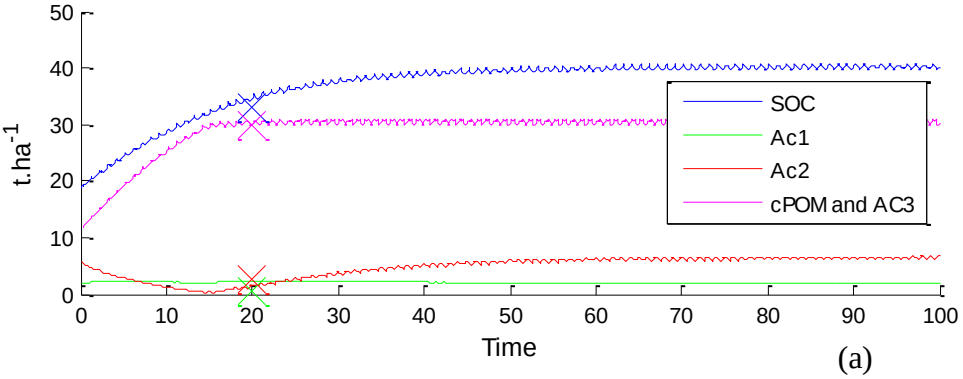
SOC
Ac1
Ac2
cPOM and AC3
t.ha-1
Time

(a)

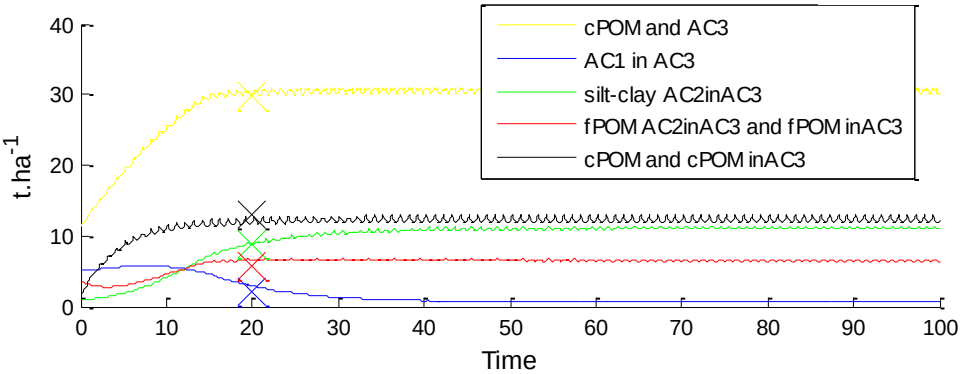
cPOM and AC3
AC1 in AC3
silt-clay AC2inAC3
fPOM AC2inAC3 and fPOM inAC3
cPOM and cPOM inAC3
t.ha-1
Time

(b) **(B)**

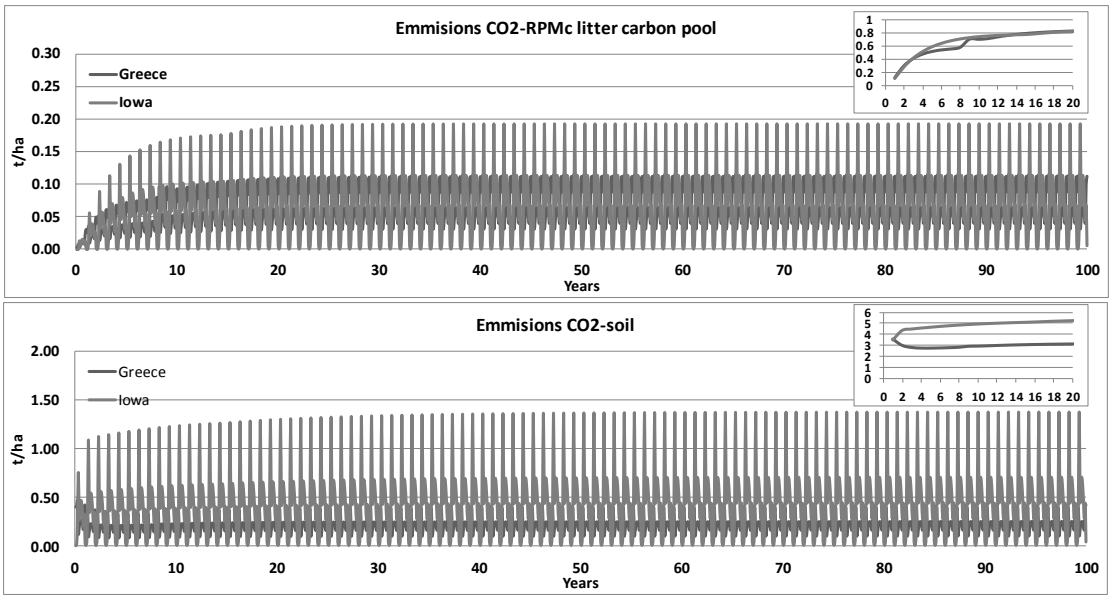
Emmisions CO2-RPMc litter carbon pool
Greece
Iowa
t/ha
Years
0.30
0.25
0.20
0.15
0.10
0.05
0.00
0 10 20 30 40 50 60 70 80 90 100
1
0.8
0.6
0.4
0.2
0
0 2 4 6 8 10 12 14 16 18 20

Emmisions CO2-soil
Greece
Iowa
t/ha
Years
2.00
1.50
1.00
0.50
0.00
0 10 20 30 40 50 60 70 80 90 100
6
5
4
3
2
1
0
0 2 4 6 8 10 12 14 16 18 20

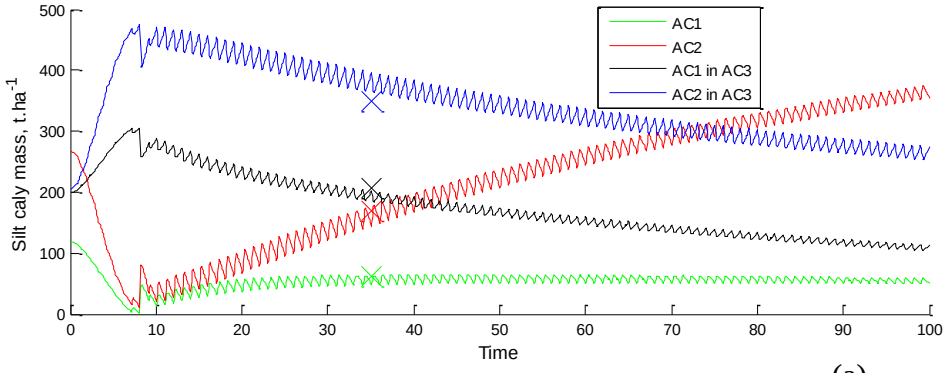
AC1
AC2
AC1 in AC3
AC2 in AC3
Silt caly mass, t.ha-1
Time

(a)

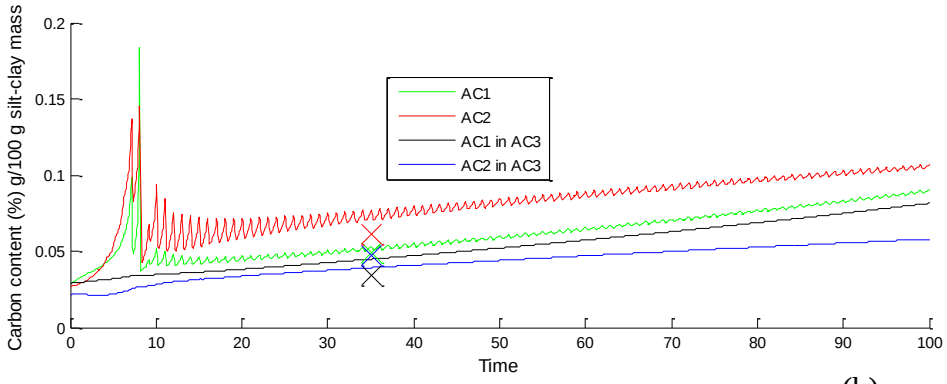
AC1
AC2
AC1 in AC3
AC2 in AC3
Carbon content (%) g/100 g silt-clay mass
Time

(b) **(A)**

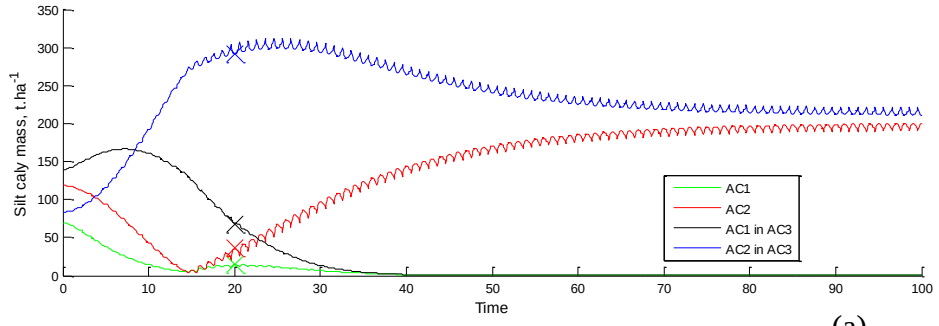
AC1
AC2
AC1 in AC3
AC2 in AC3
Silt caly mass, t.ha-1
Time

(a)

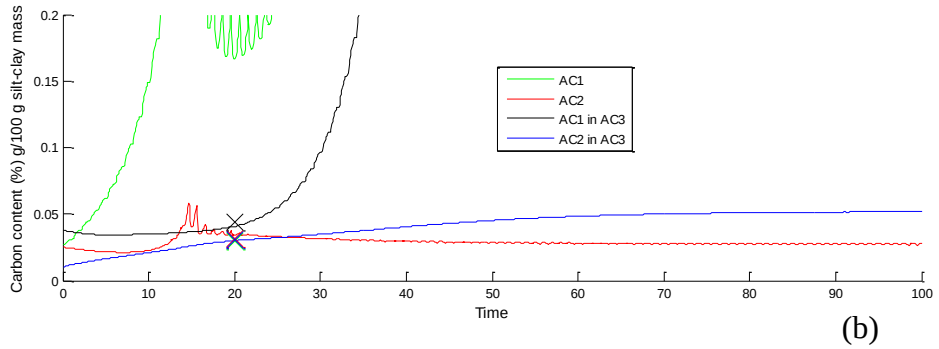
AC1
AC2
AC1 in AC3
AC2 in AC3
Carbon content (%) g/100 g silt-clay mass
Time

(b) **(B)**

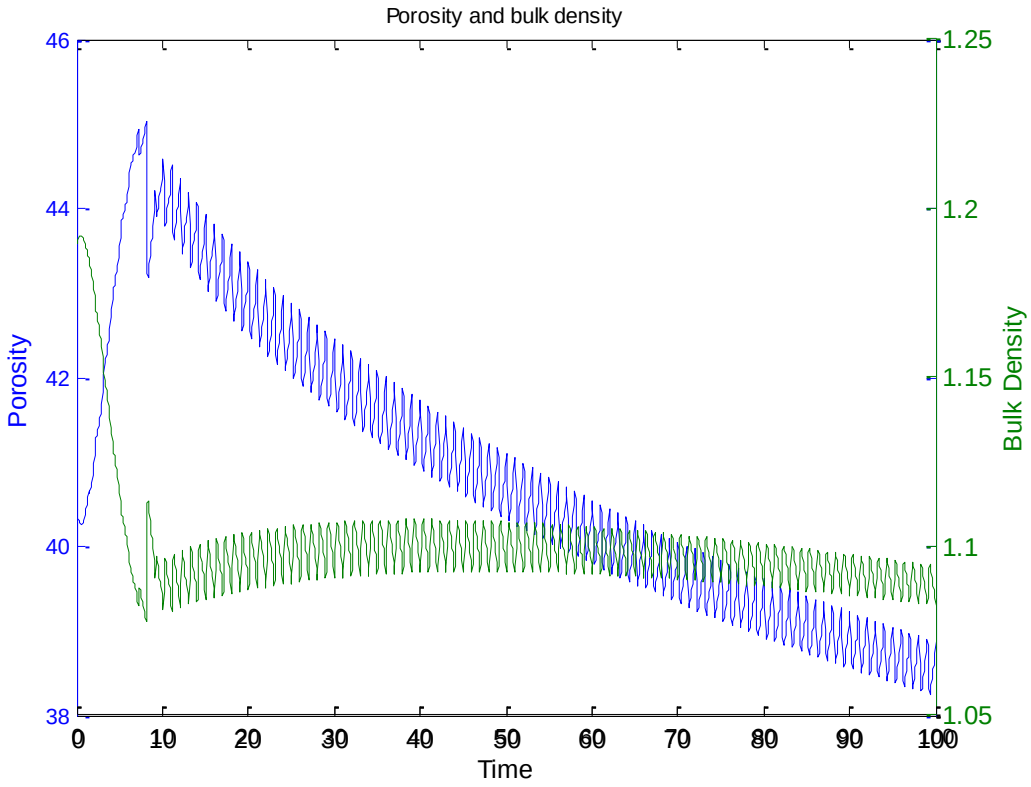
Porosity and bulk density
Porosity
Bulk Density
Time
46
44
42
40
38
1.25
1.2
1.15
1.1
1.05
0
10
20
30
40
50
60
70
80
90
100

(A)

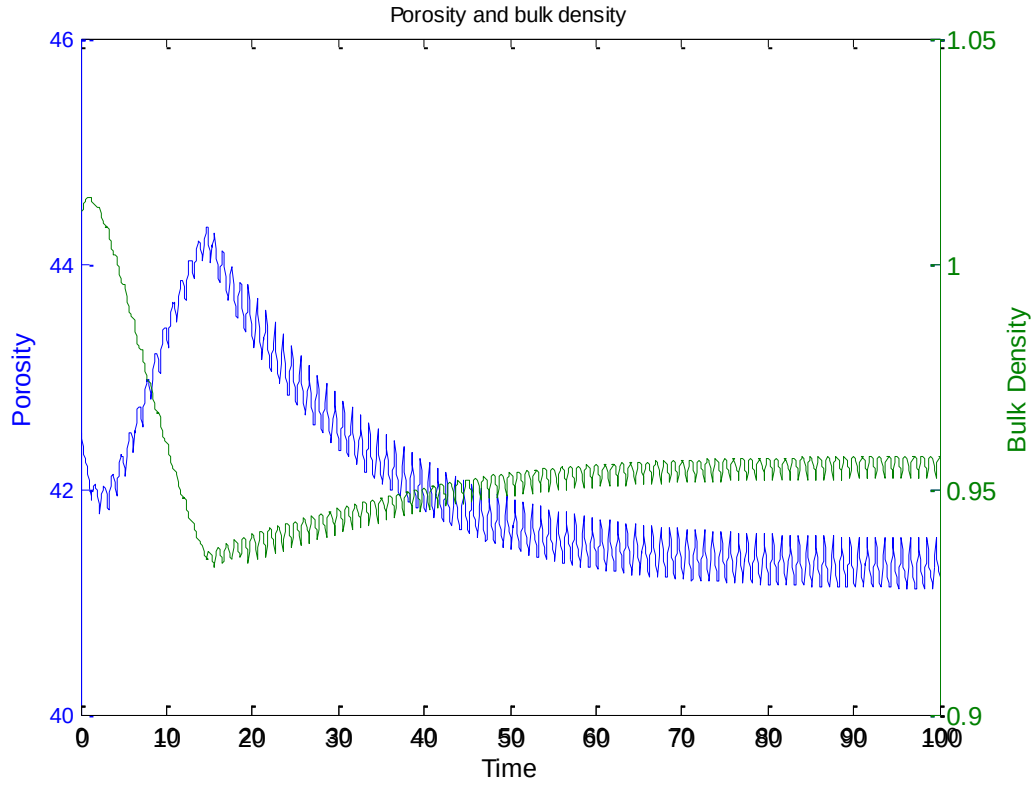
Porosity and bulk density
Porosity
Bulk Density
Time
46
44
42
40
1.05
1
0.95
0.9
0
10
20
30
40
50
60
70
80
90
100

(B)

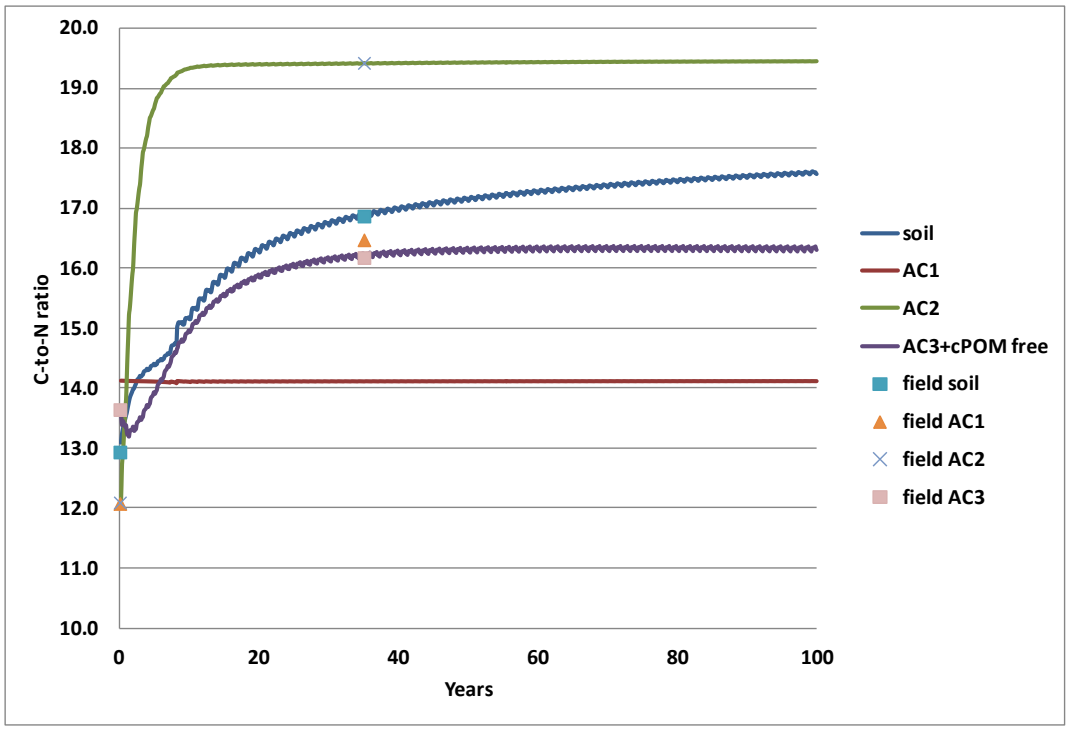
20.0
19.0
18.0
17.0
16.0
15.0
14.0
13.0
12.0
11.0
10.0
C-to-N ratio
0
20
40
60
80
100
Years
soil
AC1
AC2
AC3+cPOM free
field soil
field AC1
field AC2
field AC3

(A)

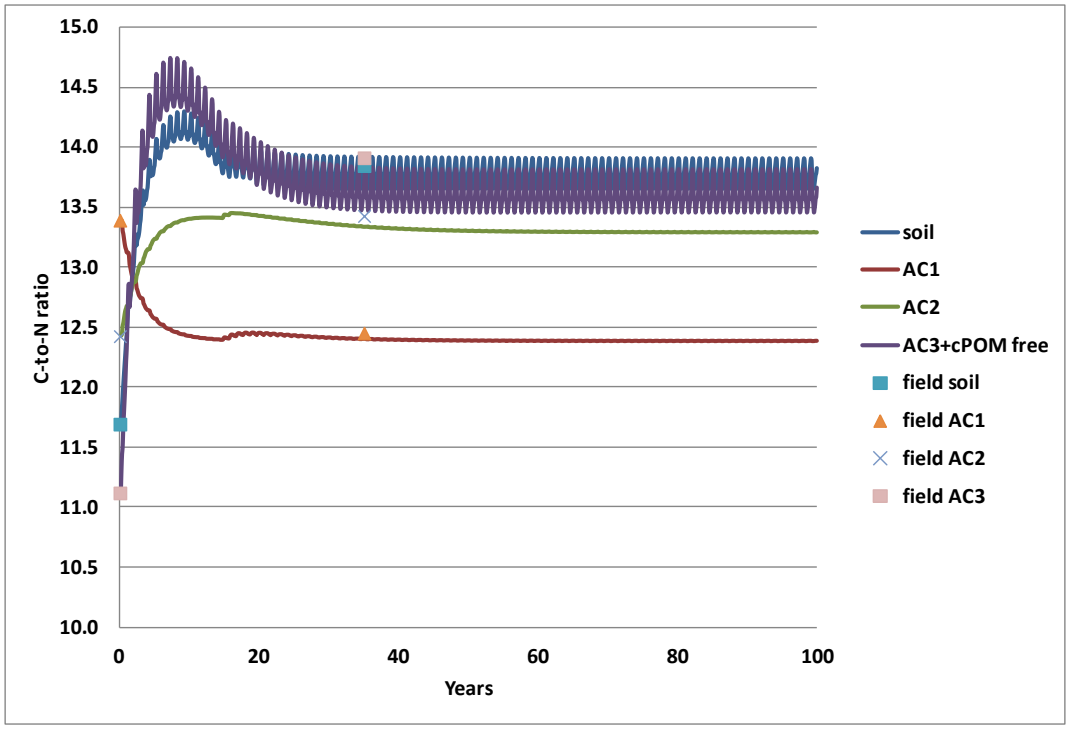
15.0
14.5
14.0
13.5
13.0
12.5
12.0
11.5
11.0
10.5
10.0
C-to-N ratio
0
20
40
60
80
100
Years
soil
AC1
AC2
AC3+cPOM free
field soil
field AC1
field AC2
field AC3

(B)

Table 1a. Field measured water stable aggregates (WSA) as well as sand corrected WSA and Carbon and Nitrogen content of the field measured pools for the Greek and the Iowa cropland and set aside fields, used for the initialization and calibration of the model, respectively (data taken by Stamati et al., (2012).

		WSA	WSA (sand free)	Carbon/Nitrogen Content									
				Aggregate		cPOM		AC1		AC2		fPOM in AC2	
	Aggregate fraction	g/100 g soil	g/100 g soil	t C/ha	t N/ha	t C/ha	t N/ha	t C/ha	t N/ha	t C/ha	t N/ha	t C/ha	t N/ha
Set aside IA	AC3 (>250 μm)	86.2	81.7	29.77	2.14	12.98	0.72	2.19	0.13	14.59	1.29	5.80	0.35
	AC2 (53-250 μm)	11.5	5.9	2.78	0.21							1.22	0.08
	AC1 (< 53 μm)	2.2	2.2	0.46	0.04								
Cropland IA	AC3 (>250 μm)	65.8	38.7	11.08	1.00	1.35	0.12	5.25	0.41	4.48	0.46	0.81	0.08
	AC2 (53-250 μm)	28.9	9.4	5.62	0.45							0.47	0.05
	AC1 (< 53 μm)	5.3	5.3	1.89	0.14								
Set aside GR	AC3 (>250 μm)	68.5	65.6	41.45	2.56	13.19	1.33	6.99	0.44	21.27	0.79	4.97	0.20
	AC2 (53-250 μm)	25.9	15.9	14.02	0.72							3.61	0.17
	AC1 (< 53 μm)	5.7	5.7	3.08	0.19								
Cropland GR	AC3 (>250 μm)	51.7	45.8	19.68	1.44	5.80	0.30	5.72	0.46	8.82	0.73	4.49	0.23
	AC2 (53-250 μm)	38.3	23.7	11.19	0.93							4.00	0.27
	AC1 (< 53 μm)	10.1	10.1	3.39	0.28								

Table 1b. Field measured silt-clay (SC) mass (t) in bulk soil and different aggregate fractions and its concentration in carbon (t C/t SC mass, %), used for the initialization and calibration of the model, respectively (data taken by Stamati et al.,2012).

	soil	AC1		AC2		AC1 in AC3		AC2 in AC3	
	SC mass, t	SC mass, t	Cons, %	SC mass, t	Cons, %	SC mass, t	Cons, %	SC mass, t	Cons, %
Set aside IA	410.7	15.0	2.7	35.8	2.5	67.7	3.8	292.1	1.0
Cropland IA	410.7	70.0	3.0	118.6	3.2	138.8	4.4	83.3	3.1
Set aside GR	790.6	62.9	4.9	169.8	6.1	207.7	3.4	350.2	4.7
Cropland GR	790.6	118.6	2.9	267.9	2.7	199.0	2.9	205.0	2.1

Table 2. Calibrated values of the rate constants and turnover time (1/rate constant - corrected with the 'abc' factors) of the model for the Greek and the Iowa cropland to set aside conversion.

			Rate Constants, 1/y		Turnover time, y	
			GR	IA	GR	IA
Fragmentation		RPM	15	20	0.1	0.2
		RPMc	0	0	-	-
		RPMc(AC3)	0.1	0.8	17.7	4.6
		DPMc(AC3)	0.5	1.0	3.5	3.6
Decomposition	plant litter pools	DPM	10.45	10	0.2	0.4
		RPM	0.305	0.5	5.8	7.3
		RPMc	0.305	0.5	5.8	7.3
		RPMf	0.305	0.5	5.8	7.3
	AC3 Aggregate type	RPMc(AC3)	0.15	0.35	11.8	10.4
		RPMf(AC3)	0.15	0.35	11.8	10.4
		DPMc(AC3)	3	3	0.6	1.2
		DPMf(AC3)	1.5	1.5	1.2	2.4
		BIO(AC1 in AC3)	0.6	0.66	2.9	5.5
		HUM(AC1 in AC3)	0.0031	0.19	570.3	19.2
		BIO(AC2 in AC3)	0.6	0.66	2.9	5.5
		HUM(AC2 in AC3)	0.0021	0.05	841.8	72.9
		RPMf(AC2 in AC3)	0.1069	0.25	16.5	14.6
		DPMf(AC2 in AC3)	1.5	1.5	1.2	2.4
	AC2 Aggregate type	BIO(AC2)	0.6	0.66	2.9	5.5
		HUM(AC2)	0.0051	0.3	346.6	12.2
		RPMf(AC2)	0.2069	0.39	8.5	9.4
		DPMf(AC2)	1.5	1.5	1.2	2.4
	AC1 Aggregate type	BIO(AC1)	0.6	0.66	2.9	5.5
		HUM(AC1)	0.0051	0.45	346.6	8.1
Macro-aggregation		RPMc(AC3)	0.6	0.65	2.9	5.6
		DPMc(AC3)	0.47	0.65	3.8	5.6
Micro-aggregation		RPMf(AC2 in AC3)	0.2	0.3	8.8	12.2
		DPMf(AC2 in AC3)	0.2	0.3	8.8	12.2
Percentages of macro-aggregation (AC3), %		RPMc	20	30		
		DPMc	20	30		
		AC1	30	35		
		AC2	30	5		
Percentages of micro-aggregation in AC3, %		RPMf(AC2 in AC3)	23.4	18		
		DPMf(AC2 in AC3)	0	0		
		AC1 in AC3	76.6	82		
Criterion for macro-aggregate destruction (DPM in AC3), %			0.15	1		
Particle density of the mineral phase, Dm			2.2	1.9		
Organic matter particle density, Dom			0.7	0.5		
Correction factor to adjust for silt-clay flow, cf		AC1	0.8	0.8		
		AC2	2.2	2.0		
		AC1 in AC3	0.16	0.5		
Distribution of sand mass in aggregates, %		f1 (AC2)	0.46	0.29		
		f2 (AC3)	0.54	0.71		

Table 3. Monthly correction factor for rate constants; the product of the rate modifying factor for temperature (a), the topsoil moisture deficit rate modifying factor (b), and the soil cover factor (c).

	GR (Crete, Greece)	IA (Iowa, USA)
January	0.733	0.004
February	0.760	0.022
March	0.901	0.216
April	0.246	0.733
May	0.340	0.274
June	0.441	0.391
July	0.488	0.448
August	0.474	0.415
September	0.410	0.310
October	0.317	0.180
November	0.776	0.272
December	0.901	0.025

Table 4. Calibrated values of the C-to-N ratio of the mechanistic N model for the Greek and the Iowa cropland to set aside conversion.

OC pool	Calibrated C-to-N ratio	
	Greece	Iowa
RPM'	42.4	50.0
DPMc	30.5	50.0
RPMc'	30.5	50.0
RPMf'	50.0	50.0
BIO_AC1'	14.0	11.3
HUM_AC1'	14.1	13.5
BIO_AC2'	6.7	10.5
HUM_AC2'	19.5	13.5
RPMf_AC2'	21.8	14.8
DPMf_AC2'	4.3	9.5
RPMc_AC3'	30.5	11.4
RPMf_AC3'	50.0	50.0
DPMc_AC3'	30.5	5.8
DPMf_AC3'	9.8	11.6
BIO_AC1_in_AC3'	14.0	14.0
HUM_AC1_in_AC3'	7.3	12.9
BIO_AC2_in_AC3'	4.1	13.5
HUM_AC2_in_AC3'	30.1	10.0
RPMf_AC2_in_AC3'	10.0	8.1
DPMf_AC2_in_AC3	18.6	12.0